



HAL
open science

Is OFDM an Optimal Multi-Carrier Modulation System in Terms of PAPR Performance?

Marwa Chafii, Jacques Palicot, Rémi Gribonval

► **To cite this version:**

Marwa Chafii, Jacques Palicot, Rémi Gribonval. Is OFDM an Optimal Multi-Carrier Modulation System in Terms of PAPR Performance?. 2015. hal-01128714v1

HAL Id: hal-01128714

<https://hal.science/hal-01128714v1>

Preprint submitted on 10 Mar 2015 (v1), last revised 30 Jun 2016 (v3)

HAL is a multi-disciplinary open access archive for the deposit and dissemination of scientific research documents, whether they are published or not. The documents may come from teaching and research institutions in France or abroad, or from public or private research centers.

L'archive ouverte pluridisciplinaire **HAL**, est destinée au dépôt et à la diffusion de documents scientifiques de niveau recherche, publiés ou non, émanant des établissements d'enseignement et de recherche français ou étrangers, des laboratoires publics ou privés.

Is OFDM an Optimal Multi-Carrier Modulation System in Terms of PAPR Performance?

Marwa Chafii, Jacques Palicot, and Rémi Gribonval

Abstract—Several Multi-Carrier Modulation systems based on different waveforms and pulse shapes are competing nowadays the conventional Orthogonal Frequency Division Multiplexing (OFDM) system based on the Fourier transform and the rectangular filter, in terms of Bit Error Rate, Spectral Efficiency, computational complexity, and other measures. In this paper, we prove analytically that, under certain constraints on the modulation scheme, conventional OFDM has an optimal Peak-to-Average Power Ratio performance.

Index Terms—Peak-to-Average Power Ratio (PAPR), Multi-Carrier Modulation (MCM), Orthogonal Frequency Division Multiplexing (OFDM), Generalized Waveforms for Multi-Carrier (GWMC), Fourier transforms.

I. INTRODUCTION

THE OFDM [1] is a Multi-Carrier Modulation (MCM) system widely used in wireless applications such as, Asymmetric Digital Subscriber Line (ADSL), Digital Audio Broadcasting (DAB), Digital Video Broadcasting-Terrestrial (DVB-T/T2), Long Term Evolution (LTE), and WiMAX, due to its resilience against frequency selective channels compared to the single modulation systems. However, the OFDM signal suffers from large amplitude variations. The fluctuations of the OFDM envelope generate non-linear distortions when we introduce the signal into the High Power Amplifier (HPA) due to the non-linearity of the HPA response. To avoid these distortions, an input back-off is needed in order to amplify the signal in the linear area of the HPA. The larger the power peaks are, the larger is the input back-off introduced and the smaller is the HPA efficiency. Therefore, the signal amplitude variations should be reduced in order to get a better HPA efficiency and minimize the power consumption. The Peak-to-Average Power Ratio has been introduced as a variable that measures the power variations of the signal.

In this paper, we show analytically that, among all MCM systems based on modulation functions that have a temporal support larger than the symbol period, OFDM is optimal in terms of PAPR performance. In addition, we prove that OFDM is not the only optimal system, but we define a large family of MCM systems with optimal PAPR performance. As an additional contribution of this paper, we show that, in order to find a new MCM system with a better PAPR performance than OFDM, the previous constraint should be relaxed, which means that the modulation functions should

have a temporal support smaller than the symbol period. To the best of our knowledge, this is the first work that gives an analytical proof of the optimality of the OFDM in terms of PAPR performance, and discusses the conditions of the validity of this optimality.

The remainder of this paper is structured as follows. In Section II, we present a state of the art of MCM systems, we define the Generalized Waveforms for Multi-Carrier (GWMC) systems considered in our derivations, and formulate the PAPR reduction problem as an optimization problem. The solution of this problem is given in Section III with the whole proof behind. To support the theoretical results, we illustrate some examples of MCM systems in Section IV. Finally, Section V concludes the paper and opens perspectives of the work.

II. PROBLEM FORMULATION

A. State of the Art

The modulation scheme of conventional OFDM is based on the Inverse Fast Fourier Transform (IFFT) and the rectangular filter. There exists other variants of the OFDM, for example, OFDM/OQAM (Offset Quadrature Amplitude Modulation) [2] which is a Filter Bank based Multi-Carrier (FBMC) system that allows a flexible selection of the pulse shaping filters [3] such as the Isotropic Orthogonal Transform Algorithm (IOTA) [4], the Extended Gaussian Functions (EGF), the PHYDYAS¹, and the Hermite, in order to reduce side lobes without using guard bands in contrast to the conventional OFDM. Oversampled OFDM is another variant of OFDM, which can use a well-localized pulse shape to fight against time and frequency dispersion [5]. Non-Orthogonal Frequency Division Multiplexing (NOFDM) [6] is an MCM system that does not have any restriction about the distance between pulses in the time-frequency (TF) plane, and the design of the pulse shape, which leads to a better bandwidth efficiency, while the TF location and the shape of the pulses for conventional OFDM are strictly defined. Previous MCM systems can be treated as subclasses of the Generalized Multi-Carrier (GMC) system which includes OFDM, NOFDM, FBMC [7] and other variants as explained in the taxonomy proposed in [8]. For the different pulse shaping filters, the reader can refer to [9] that defines and gives the analytical expression and characteristics of the most known prototype filters in the literature.

Instead of modulating the signal with the IFFT, other

M. Chafii and J. Palicot are with the CentraleSupélec/IETR, 35576 Cesson-Sévigné, France (e-mail: {marwa.chafii, jacques.palicot} @supelec.fr).

R. Gribonval is with Inria Rennes-Bretagne, 35042 Rennes Cedex, France (e-mail: remi.gribonval@inria.fr)

¹Physical Layer For Dynamic Spectrum Access And Cognitive Radio, more details on <http://www.ict-phydyas.org/>

transforms can be used. In [10], the author introduces the Hadamard transform and Phi transform for MCM applications, than compares them with conventional OFDM. In the literature, and for different applications, we find also MCM systems based on the Inverse Discrete Cosine Transform (IDCT) [11] [12], The Inverse Discrete Wavelet Transform (IDWT) [13], the Inverse Wavelet Packet Transform (IWPT) [14], and the Inverse Slantlet Transform (ISLT) [15]. Nowadays, many MCM systems are competing conventional OFDM in terms of Out-Of-band (OOB) radiation, Bit Error Rate (BER), computational complexity, and other measures. In fact, the flexibility in the choice of the pulse shape in GMC systems allows high spectral efficiency combined with lower OOB radiation than conventional OFDM [16]. It has been also showed that MCM systems based on Hadamard transform are more suitable for optical communications than OFDM at short distance transmission, in terms of computational complexity [17]. In [18], the MCM scheme based on the IDCT has been proved better than the one based on the IFFT (OFDM) in terms of BER under certain channel conditions. Hereafter, we give a proof and a discussion about the PAPR optimality of conventional OFDM. The early work in this context goes back to the study of A. Skrzypczak et al. for the OFDM/OQAM and the oversampled OFDM [19]. They show analytically that the PAPR performance for the latest two MCM systems based on different pulse shapes is not better than the conventional OFDM based on the rectangular pulse shape. Based on simulation results, A. Kliks [20] notices that, when simulating the Complementary Cumulative Distribution Function (CCDF) of the PAPR for the GMC signal for different pulses, the lowest values are obtained for the rectangular pulse. In this work, we consider a more general MCM system named GWMC, which is based on a larger choice of modulation schemes and we give an analytical study to prove that, within this family of modulation schemes, the IFFT and the rectangular filter are an optimal modulation scheme in terms of PAPR performance.

B. Notation: the GWMC Model

The notations used in this paper are as follows: M denotes the number of carriers. $C_{m,n}$ stands for the input symbol index n modulated by the carrier index m and let σ_C^2 be its variance. T is the GWMC symbol period. The modulation transform and the pulse shaping filter are modeled by a single function denoted by $g_m \in L^2(\mathbb{R})$ (the space of square integrable functions). The GWMC transmitted signal is expressed as

$$X(t) = \sum_{n \in \mathbb{Z}} \sum_{m=0}^{M-1} C_{m,n} \underbrace{g_m(t - nT)}_{g_{m,n}(t)}. \quad (1)$$

C. Optimization Problem associated to PAPR reduction

We consider a GWMC system based on a family of modulation functions $(g_m)_{m \in [0, M-1]}$ that satisfy the following conditions

$$A = \min_{m,t} \sum_{n \in \mathbb{Z}} |g_m(t - nT)|^2 > 0, \quad (2)$$

$$\text{and } B = \max_{m,t} \sum_{n \in \mathbb{Z}} |g_m(t - nT)| < +\infty \quad (3)$$

Eq.(2) means that the translated versions of every carrier g_m are overlapping in time. The temporal support of the waveform g_m does not vanish in the symbol period T . Eq.(3) means that the functions g_m have a temporal decay.

In the discrete time context, let P be the number of samples considered in the symbol period T , and we define the discrete-time PAPR of the GWMC signal as follows

$$\text{PAPR}_d = \frac{\max_{k \in [0, P-1]} |X(k)|^2}{P_{mean}} \quad (4)$$

$$P_{mean} = \lim_{K \rightarrow +\infty} \frac{1}{2K+1} \sum_{k=-K}^K E(|X(k)|^2) \quad (5)$$

The index d corresponds to the discrete-time context. The mean power P_{mean} is defined over an infinite integration time, because our scenario assumes an infinite transmission time, but the observation is limited to a single GWMC symbol. The CCDF of the PAPR for the GWMC signal is approximated by the following formula [21]

$$\Pr(\text{PAPR}_d \geq \gamma) \approx 1 - \prod_{k \in [0, P-1]} [1 - e^{-x(k)\gamma}], \quad (6)$$

$$\text{with } x(k) = \frac{\sum_{m=0}^{M-1} \|g_m\|^2}{P \sum_{n \in \mathbb{Z}} \sum_{m=0}^{M-1} |g_m(k - nP)|^2}.$$

The norm $\|g_m\|$ of the function g_m is defined as: $\|g_m\|^2 = \int_{-\infty}^{+\infty} |g_m(t)|^2 dt$. Reducing the PAPR means reducing its CCDF, which is the probability that the PAPR exceeds a defined value γ . Based on this fact, we showed in our previous work [22], that the PAPR reduction problem can be formulated as the following constrained Optimization Problem

Optimization Problem (OP).

$$\begin{aligned} & \underset{(g_m)_{m \in [0, M-1]}}{\text{maximize}} && \int_0^T \ln(1 - e^{-\frac{-\gamma \sum_{m=0}^{M-1} \|g_m\|^2}{P \sum_{n \in \mathbb{Z}} \sum_{m=0}^{M-1} |g_m(t - nT)|^2}}) dt, \\ & \text{subject to} && \exists A, B \in \mathbb{R} \\ & && A = \min_{m,t} \sum_{n \in \mathbb{Z}} |g_m(t - nT)|^2 > 0, \\ & \text{and} && B = \max_{m,t} \sum_{n \in \mathbb{Z}} |g_m(t - nT)| < +\infty \end{aligned}$$

The quantity that we want to maximize is equivalent to minimizing the CCDF of the PAPR. For a certain value of γ , we want to minimize the probability that the PAPR exceeds this value of γ .

III. MAIN RESULTS

A. Replacing OP with a Simpler Problem

In order to characterize the optima of OP, we first do some simplifications. We start by noticing that the functions $(g_m)_{m \in [0, M-1]}$ perform the same role and only the sum

$\sum_{n \in \mathbb{Z}} \sum_{m=0}^{M-1} |g_{m,n}(t)|^2$ is involved in the maximized quantity, the maximization can thus be performed over only one non-negative function $f(t)$, such that

$$f(t) = \sum_{m=0}^{M-1} \sum_{n \in \mathbb{Z}} |g_{m,n}(t)|^2, \quad (7)$$

Eq.(2) implies that $\exists a = MA$ such that $f(t) \geq a > 0$. Similarly, Eq.(3) implies that $f \in L^\infty$, where L^∞ is the space of essentially bounded functions. Moreover,

$$\begin{aligned} \int_0^T f(\tau) d\tau &= \int_0^T \sum_{m=0}^{M-1} \sum_{n \in \mathbb{Z}} |g_m(t - nT)|^2 dt \\ &= \sum_{m=0}^{M-1} \sum_{n \in \mathbb{Z}} \int_{nT}^{nT+T} |g_m(t - nT)|^2 dt \\ &= \sum_{m=0}^{M-1} \int_{-\infty}^{+\infty} |g_m(t)|^2 dt \\ &= \sum_{m=0}^{M-1} \|g_m\|^2. \end{aligned} \quad (8)$$

The quantity that we want to maximize is then expressed as

$$\begin{aligned} \underset{f \in L^\infty}{\text{maximize}} \quad & \beta(f) = \int_0^T \ln(1 - e^{-\frac{\gamma \int_0^T f(\tau) d\tau}{P f(t)}}) dt. \quad (9) \\ \text{subject to} \quad & \exists a \text{ such that} \\ & f(t) \geq a > 0. \end{aligned}$$

Remark 1. It is worth noting that the expression of $\beta(f)$ does not change if we multiply the function $f(t)$ by a scalar: for all $\lambda \in \mathbb{R}^{*+}$, we have

$$\beta(\lambda f) = \beta(f). \quad (10)$$

It follows that if the problem in Eq.(9) has an optimal solution, then there exists an infinite set of optimal solutions obtained by scaling the first solution.

Moreover, denoting $\tilde{f}(t) = f(Tt)$, we have

$$\beta(f) = T \int_0^1 \ln(1 - e^{-\frac{\gamma T \int_0^1 \tilde{f}(\tau) d\tau}{P \tilde{f}(t)}}) dt \quad (11)$$

$$=: T \tilde{\beta}(\tilde{f}), \quad (12)$$

$$\text{and} \quad \tilde{f} \geq a > 0. \quad (13)$$

Maximizing $\tilde{\beta}$ with respect to \tilde{f} is then equivalent to maximizing β with respect to f .

From Remark.1, we can still simplify the expression of $\tilde{\beta}$ by considering the following normalization

$$\frac{\gamma T}{P} \int_0^1 \tilde{f}(\tau) d\tau = 1. \quad (14)$$

This corresponds to considering $\tilde{f}(t) = C f(Tt)$, such that $C = \frac{P}{\gamma \sum_{m=0}^{M-1} \|g_m\|^2}$. The condition Eq.(14) is also considered as another constraint of the OP. The new expression of $\tilde{\beta}$ is then

$$\tilde{\beta}(\tilde{f}) = \int_0^1 \ln(1 - e^{-\frac{1}{\tilde{f}(t)}}) dt. \quad (15)$$

B. Theoretical Analysis

We define the following convex subsets of L^∞

- $F := \left\{ f : [0, 1] \rightarrow \mathbb{R}^{*+} \text{ such that } \int_0^1 f(\tau) d\tau = \frac{P}{\gamma T} \right\}$,
- $F_a := F \cap \{ f : [0, 1] \rightarrow \mathbb{R}^{*+} \text{ such that } f \geq a \}$,
- $F_+ := \bigcup_{a>0} F_a$.

We consider here the optimization problem in Eq.(15) with the constraint Eq.(13)-(14). To characterize its optima, we first recall the definition of its stationary points.

Definition 1. We say that a function $f^* \in F_a$ is a stationary point of $\tilde{\beta}$ defined in Eq.(15) under the constraint in Eq.(13)-(14) if and only if: For any $\phi \in L^1 \cap L^\infty([0, 1])$ such that

$$\int_0^1 \phi(t) dt = 0 \quad (16)$$

we have

$$\left. \frac{d\tilde{\beta}(f^* + \epsilon\phi)}{d\epsilon} \right|_{\epsilon=0} = 0. \quad (17)$$

L^1 is the space of Lebesgue integrable functions. Notice that for all ϕ satisfying Eq.(16), $f^* + \epsilon\phi$ satisfies Eq.(14). For small enough ϵ , $f^* + \epsilon\phi$ also satisfies Eq.(13).

The solution of the optimization problem is organized as follows

Lemma 1.

Let f_0 be the unique solution to the equation $1 - 2f_0 + 2f_0 e^{\frac{1}{f_0}} = 0$. $\forall f \in F_{f_0}$, $\forall \phi \in L^1 \cap L^\infty([0, 1])$ such that Eq.(16) holds, we have

$$\left. \frac{d^2 \tilde{\beta}(f^* + \epsilon\phi)}{d\epsilon^2} \right|_{\epsilon=0} \leq 0. \quad (18)$$

Lemma 2.

The constant $f^* = \frac{P}{\gamma T}$ is the unique stationary point of $\tilde{\beta}$ defined in Eq.(15) over the set F_+ .

Corollary 1. The constant $f^* = \frac{P}{\gamma T}$ is a global maximum of $\tilde{\beta}$ in Eq.(15) under the constraint in Eq.(13)-(14) over the set F_{f_0} .

Hereafter, the proofs are presented.

1) *Proof of Lemma 1:* Let f_0 be the unique solution to the equation $1 - 2f_0 + 2f_0 e^{\frac{1}{f_0}} = 0$, and $f \in F_{f_0}$. Since $f \in F_{f_0}$ and ϕ is bounded, there is $\epsilon_0 > 0$ such that for any ϵ such that $|\epsilon| \leq \epsilon_0$, the constraint in Eq.(13) holds. We

now explicit the derivatives involved in Eq.(17). We have

$$\begin{aligned}
 \tilde{\beta}(f + \epsilon\phi) &= \int_0^1 \ln(1 - e^{\frac{-1}{f(t) + \epsilon\phi(t)}}) \\
 \frac{d\tilde{\beta}(f + \epsilon\phi)}{d\epsilon} &= \int_0^1 \frac{\frac{-\phi(t)}{(f(t) + \epsilon\phi(t))^2} e^{\frac{-1}{(f(t) + \epsilon\phi(t))}}}{1 - e^{\frac{-1}{(f(t) + \epsilon\phi(t))}}} dt \\
 \frac{d^2\tilde{\beta}(f + \epsilon\phi)}{d\epsilon^2} &= \int_0^1 \frac{d}{d\epsilon} \left(\frac{\frac{-\phi(t)}{(f(t) + \epsilon\phi(t))^2} e^{\frac{-1}{(f(t) + \epsilon\phi(t))}}}{1 - e^{\frac{-1}{(f(t) + \epsilon\phi(t))}}} \right) dt \\
 &= - \int_0^1 \frac{(\frac{-2\phi^2}{(f + \epsilon\phi)^3} + \frac{\phi^2}{(f + \epsilon\phi)^4}) e^{\frac{-1}{f + \epsilon\phi}} (1 - e^{\frac{-1}{f + \epsilon\phi}})}{(1 - e^{\frac{-1}{f + \epsilon\phi}})^2} \\
 &\quad + \int_0^1 \frac{(\frac{\phi}{(f + \epsilon\phi)^2} e^{\frac{-1}{f + \epsilon\phi}}) (\frac{-\phi}{(f + \epsilon\phi)^2} e^{\frac{-1}{f + \epsilon\phi}})}{(1 - e^{\frac{-1}{f + \epsilon\phi}})^2} dt \\
 \left. \frac{d^2\tilde{\beta}(f + \epsilon\phi)}{d\epsilon^2} \right|_{\epsilon=0} &= - \int_0^1 \frac{(\frac{-2\phi^2}{f^3} + \frac{\phi^2}{f^4}) e^{\frac{-1}{f}} (1 - e^{\frac{-1}{f}})}{(1 - e^{\frac{-1}{f}})^2} \\
 &\quad - \int_0^1 \frac{\frac{\phi^2}{f^4} e^{\frac{-2}{f}}}{(1 - e^{\frac{-1}{f}})^2} \\
 \left. \frac{d^2\tilde{\beta}(f + \epsilon\phi)}{d\epsilon^2} \right|_{\epsilon=0} &= - \underbrace{\int_0^1 \frac{\frac{\phi^2}{f^4} e^{\frac{-1}{f}}}{(1 - e^{\frac{-1}{f}})^2}}_{\geq 0} \underbrace{(1 - 2f + 2fe^{\frac{-1}{f}})}_{s(f)} dt.
 \end{aligned} \tag{19}$$

In Appendix, we show that the function s is positive when f is greater than a certain value f_0 satisfying $s(f_0) = 0$. Then, we conclude that, for all $f \in F_{f_0}$,

$$\frac{d^2\tilde{\beta}(f^* + \epsilon\phi)}{d\epsilon^2} \leq 0. \tag{20}$$

2) *Proof of Lemma 2:* Consider $f^* \in F_+$. Let $\phi \in L^1 \cap L^\infty([0, 1])$ be such that Eq.(16) holds. We have from Eq.(19)

$$\left. \frac{d\tilde{\beta}(f + \epsilon\phi)}{d\epsilon} \right|_{\epsilon=0} = \int_0^1 \frac{\frac{-\phi(t)}{f^2(t)} e^{\frac{-1}{f(t)}}}{1 - e^{\frac{-1}{f(t)}}} dt,$$

Defining

$$\psi(t) = \frac{e^{\frac{-1}{f^*(t)}}}{[1 - e^{\frac{-1}{f^*(t)}}] f^{*2}(t)}, \tag{21}$$

it follows that Eq.(17) is equivalent to,

$$\int_0^1 \phi(t) \psi(t) dt = 0. \tag{22}$$

At this stage, we can check that if $f^* = \frac{P}{\gamma T}$ then $\psi(t) = c_0$ does not depend on t , hence we have established that for any $\phi(t)$ satisfying Eq.(16), we must have: $\int_0^1 \psi(t) \phi(t) dt = c_0 \int_0^1 \phi(t) dt = 0$, i.e. Eq.(17) holds. This shows, as claimed, that $f^* = \frac{P}{\gamma T}$ is a stationary point of Eq.(15) under the constraint Eq.(13)-(14). We will now prove the converse.

Assume now that $f^* \in F_+$ is a stationary point of Eq.(15) with the constraint Eq.(13)-(14). What we have just established is that Eq.(22) must hold for all ϕ that satisfies Eq.(16). ψ is

then orthogonal to all the zero mean functions $\phi \in L^1 \cap L^\infty$. Thus, ψ is a constant c_0 , i.e.

$$\frac{e^{\frac{-1}{f^*(t)}}}{[1 - e^{\frac{-1}{f^*(t)}}] f^{*2}(t)} = c_0. \tag{23}$$

Hence, $\exists c_0 \in \mathbb{R}$ such that $\forall t \in [0, 1]$ $f^*(t)$ belongs to the set of solutions of the equation $h(f) = c_0$ with

$$h(f) = \frac{e^{\frac{-1}{f}}}{[1 - e^{\frac{-1}{f}}] f^2}. \tag{24}$$

To conclude that f^* itself be constant, we now analyse the variations of the function $h(f)$.

The simulation of $h(f)$ in Figure.1, shows that for a certain

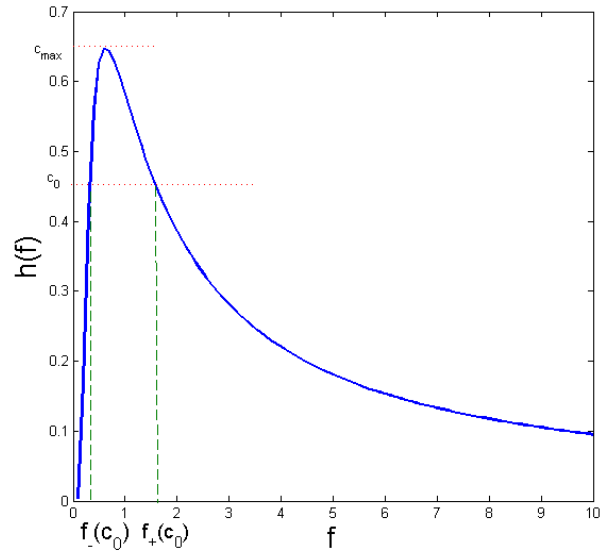


Figure 1: The curve of the function $h(f)$

value c_0 , the line of equation $h(f) = c_0$ cuts the curve of the function h in a single point which coincides with the maximum value of h that we note c_{\max} , and two distinct points when c_0 is less than c_{\max} . When c_0 is greater than c_{\max} the line does not cut the curve of h .

Thus, the set S_h of solutions of Eq.(23) can be expressed as

$$S_h = \begin{cases} f_+(c_0), f_-(c_0) & \text{if } 0 < c_0 \leq c_{\max}, \\ \emptyset & \text{if } c_0 > c_{\max}. \end{cases} \tag{25}$$

Note that when $c_0 = c_{\max}$, we have $f_+(c_0) = f_-(c_0)$.

$f_+(c_0)$ is the greater solution, and $f_-(c_0)$ is the smaller one ($f_-(c_0) \leq f_+(c_0)$).

The following property summarizes what we have established so far

Property 1. Let $f^* \in F_+$ be a stationary point of $\tilde{\beta}$, under the constraint Eq.(13)-(14). There exists a constant $c_0 \in [0, c_{\max}]$, a set \mathcal{A}_+ and a set $\mathcal{A}_- = [0, 1] \setminus \mathcal{A}_+$ such that

$$f_{|\mathcal{A}_+} = f_+(c_0), \quad \text{and} \quad f_{|\mathcal{A}_-} = f_-(c_0). \tag{26}$$

$f_{|\mathcal{A}_+}$ ($f_{|\mathcal{A}_-}$ respectively) is the restriction of the function f over the set $\mathcal{A}_+ \subset [0, 1]$ ($\mathcal{A}_- \subset [0, 1]$ respectively).

Table I: Solutions of Eq.(23) for different values of c_0

c_0	$f_-(c_0)$	$f_+(c_0)$
0.64	0.720	00.72
0.62	0.510	00.83
0.60	0.450	00.90
0.50	0.360	01.34
0.40	0.300	01.90
0.30	0.250	02.76
0.20	0.210	04.46
0.10	0.170	09.48
0.05	0.145	19.50
0.02	0.091	49.49
0.01	0.085	99.49

Table II: Variations of f_+ , f_- and $\frac{1}{f_+ - f_-}$ as a function of c_0

c_0	0	c_{\max}
f_+	$+\infty$	f_{\max}
f_-	0	f_{\max}
$\frac{1}{f_+ - f_-}$	0	$+\infty$

Corollary 2. *The Lebesgue measure of the interval \mathcal{A}_+ can be expressed as*

$$\tilde{L}_{\mathcal{A}_+(c_0)} = \frac{\frac{P}{\gamma T} - f_-(c_0)}{f_+(c_0) - f_-(c_0)} \in [0, 1] \quad (27)$$

In fact, from Eq.(14) and Property.1, we have

$$\tilde{L}_{\mathcal{A}_+}(c_0)f_+(c_0) + (1 - \tilde{L}_{\mathcal{A}_+})f_-(c_0) = \frac{P}{\gamma T} \quad (28)$$

$$\tilde{L}_{\mathcal{A}_+}(c_0)(f_+(c_0) - f_-(c_0)) = \frac{P}{\gamma T} - f_-(c_0). \quad (29)$$

Property 2. *Let $f^* \in F_+$ be a stationary point of $\tilde{\beta}$, under the constraint Eq.(13)-(14). Then, the value of c_0 solves the following optimization problem*

$$\begin{aligned} \underset{c_0}{\text{maximize}} \quad & \tilde{\beta}(c_0) = \tilde{L}_{\mathcal{A}_+}(c_0) \ln(1 - e^{-\frac{1}{f_+(c_0)}}) \\ & + (1 - \tilde{L}_{\mathcal{A}_+}(c_0)) \ln(1 - e^{-\frac{1}{f_-(c_0)}}), \\ \text{subject to} \quad & \tilde{L}_{\mathcal{A}_+}(c_0) \in [0, 1]. \end{aligned}$$

Numerical Results: Table I shows for each value of c_0 the set of solutions S_h of Eq.(23). As we can see, $f_-(c_0)$ is an increasing function of c_0 and $f_+(c_0)$ is a decreasing function of c_0 , we can resume these conclusions in Table II.

Now, we should study the variations of $\tilde{\beta}(c_0)$, which depend on the monotonicity of $\tilde{L}_{\mathcal{A}_+}$. We have $\frac{P}{\gamma T} \geq f_-$ since $\tilde{L}_{\mathcal{A}_+}$ is positive, so we cannot decide directly on the monotonicity of $\tilde{L}_{\mathcal{A}_+}$, because it is the product of a positive decreasing function $c_0 \mapsto \frac{P}{\gamma T} - f_-(c_0)$ and a positive increasing function $c_0 \mapsto \frac{1}{f_+(c_0) - f_-(c_0)}$. Therefore, we simulate the variations of $\tilde{L}_{\mathcal{A}_+}$ and $\tilde{\beta}(c_0)$ as depicted in Fig.2, 3.

To maximize $\tilde{\beta}$ we should minimize $\tilde{L}_{\mathcal{A}_+}$ under the constraint of $0 \leq \tilde{L}_{\mathcal{A}_+} \leq 1$. For $\tilde{L}_{\mathcal{A}_+} = 0$, we have $f_- = \frac{P}{\gamma T}$ and

Table III: Values of γ_{\max} for different values of M for the OFDM system

M	8	16	32	64	126	256	512	1024
γ_{\max} , in dB	11	14	17	20	23	26	29	32

$\tilde{\beta}^* = \ln(1 - e^{-\frac{\gamma T}{P}})$. Thus, f^* takes a single value f_- and $f^* = \frac{P}{\gamma T}$. To conclude, for $f^* \in F_+$ a stationary point of $\tilde{\beta}$ under the constraint in (Eq.14), we have $f^* = \frac{P}{\gamma T}$. This concludes the proof of Lemma 2.

3) *Proof of Corollary 1:* From Lemma 1, $\tilde{\beta}$ is a concave function over the convex set F_{f_0} . Then, its local maximum is global maximum over F_{f_0} [23]. From Lemma 2, $f^* = \frac{P}{\gamma T}$ is a global maximum of $\tilde{\beta}$ over F_{f_0} .

C. Discussion

The condition $\forall t, \tilde{f}(t) \geq f_0$ expressed in the previous results corresponds to the following constraint in terms of the family of modulation functions $(g_m)_{m \in [0, M-1]}$:

$$\forall t \quad \gamma \leq \frac{P \sum_{m=0}^{M-1} \sum_{n \in \mathbb{Z}} |g_{m,n}(t)|^2}{f_0 \sum_{m=0}^{M-1} \|g_m\|^2}, \quad (30)$$

which means that our results are valid for the values of γ less than a threshold value γ_{\max} . Let us consider the OFDM system for example: the modulus of the waveform g_m corresponds to the rectangular filter supposed of unit energy ($\|g_m\|^2 = 1$), and $P = M$ for critical sampling. The threshold value is expressed then as $\gamma_{\max} = \frac{M}{f_0}$. Table III shows the values of γ_{\max} , the threshold of the validity of our results, in function of the number of carriers M , for the OFDM system. In practice, the PAPR does not reach these values of γ for the corresponding number of carriers M .

Based on the previous theoretical results, we deduce some properties that can predict the behaviour of the PAPR distribution function for GWMC systems compared to the OFDM system.

Property 3. (Sufficient condition for optimality)

Any GWMC system satisfying Eq.(2)-(3) such that $\sum_{m=0}^{M-1} \sum_{n \in \mathbb{Z}} |g_m(t - nT)|^2$ is constant over time, has locally optimal PAPR performance, and globally optimal PAPR performance among all GWMC systems satisfying Eq.(2)-(3) such that Eq.(30) holds.

Corollary 3. (Optimality of conventional OFDM)

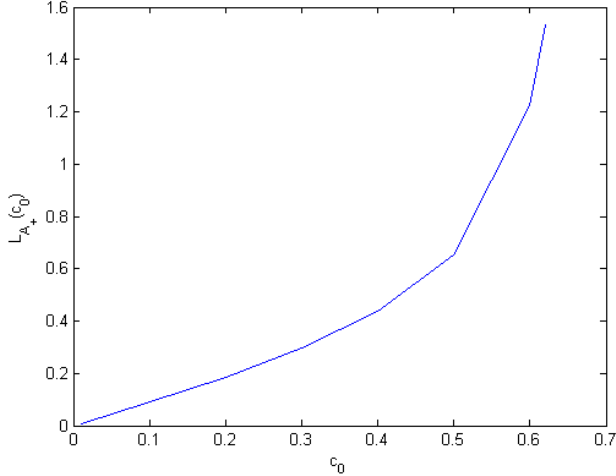
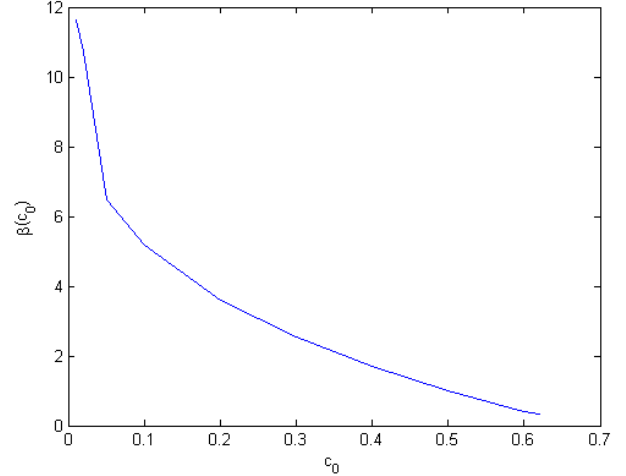
The OFDM achieves optimal PAPR performance among all GWMC systems satisfying Eq.(2)-(3) such that Eq.(30) holds. So does the Walsh-Hadamard system.

Example: See Subsection IV-A.

Corollary 4.

Any GWMC system satisfying Eq.(2)-(3) and Eq.(30) such that $\sum_{m=0}^{M-1} \sum_{n \in \mathbb{Z}} |g_m(t - nT)|^2$ is not constant over time has worse PAPR performance than OFDM.

Example: See Subsection IV-B.

Figure 2: The curve of the function $\tilde{L}_{A^+}(c_0)$.Figure 3: The curve of the function $\tilde{\beta}(c_0)$.

Property 4. To construct a GWMC system with better PAPR performance than OFDM, one must choose the modulation functions so that at least one of the following conditions holds:

- i) the system fails to satisfy Eq.(2): this means that the temporal support of at least one modulation function must be less or equal than the symbol period.
- ii) the system fails to satisfy Eq.(30).

In fact, the result in Corollary.4 is true when the constraints in Eq.(2) and Eq.(3) and Eq.(30) hold. In practice, all the waveforms has to satisfy Eq.(3), because they have a finite temporal support and they are bounded. Then, we have

- i) if a family of functions $(g_m)_{m \in \llbracket 0, M-1 \rrbracket}$ does not satisfy Eq.(2), that means that there exists at least an index $m_0 \in \llbracket 0, M-1 \rrbracket$ such that g_{m_0} has a temporal support less than the symbol period, which means that its amplitude vanishes at least in a time interval, then g_{m_0} has a larger frequency support and then a worse frequency localization. This is due to the Time Frequency Localization (TFL), which is limited by the Heisenberg uncertainty principle². Thus, we are led to a trade-off between frequency localization and PAPR performance. Example: See Subsection IV-C.

- ii) if Eq.(30) is not satisfied, that means that, for a defined GWMC system $(g_m)_{m \in \llbracket 0, M-1 \rrbracket}$, the PAPR is compared to the values of $\gamma > \gamma_{\max}$. Knowing that the PAPR is bounded by a multiple factor of M [25]: $\text{PAPR}_{\text{bound}} = \frac{\max_{m,n} |C_{m,n}|^2 B^2}{\sigma_c^2 A} M$, the CCDF is then equal to zero when $\gamma > \text{PAPR}_{\text{bound}}$. Thus, the analysis is restricted to the values of γ between γ_{\max} and $\text{PAPR}_{\text{bound}}$, which does not represent an interval of interest, since in practice the PAPR does not reach these large values of γ .

²Or sometimes the Heisenberg-Gabor theorem, it states that a function cannot be both time-limited and band-limited (a function and its Fourier transform cannot both have bounded domain). Then, one cannot simultaneously sharply localize a signal in both the time domain and the frequency domain. More details can be found in [24]

IV. APPLICATIONS

In order to illustrate our results, we consider three variants of the OFDM, that are based on different families of modulation functions, and we simulate the CCDF of their PAPR. A comparison in terms of PAPR performance, between each variant and the conventional OFDM, is presented.

A. Walsh-Hadamard-MC (WH-MC)

Instead of using the IFFT for the modulation, we can use Inverse Walsh-Hadamard Transform (IWHT). Then, the family of the modulation functions is expressed as:

$$g_m(k) = W_{q,p}(k)$$

$W_{q,p}$ are the Walsh functions and are columns of Hadamard matrix of dimension $M = 2^Q$, which is defined by the recursive formula:

$$H(2^1) = \begin{pmatrix} 1 & 1 \\ 1 & -1 \end{pmatrix} \quad (31)$$

$$H(2^2) = \begin{pmatrix} 1 & 1 & 1 & 1 \\ 1 & -1 & 1 & -1 \\ 1 & 1 & -1 & -1 \\ 1 & -1 & -1 & 1 \end{pmatrix}, \quad (32)$$

and for $2 \leq q \leq Q$:

$$H(2^q) = \begin{pmatrix} H(2^{q-1}) & H(2^{q-1}) \\ H(2^{q-1}) & -H(2^{q-1}) \end{pmatrix} = H(2) \otimes H(2^{q-1}), \quad (33)$$

where \otimes denotes the Kronecker product.

Note that the Hadamard matrix consists only of +1 and -1 entries, that is why the implementation has a simple structure featuring only additions and subtractions. In fact, IWHT can be implemented using the radix-2 algorithm, which means that there are only $M \log_2 M$ complex additions required [26].

Fig.4 depicts the shape of the first Walsh functions. As we can notice, all the functions have the same modulus and this modulus is constant over time. From Corollary.3, WH-MC has the same PAPR optimal performance as the conventional OFDM.

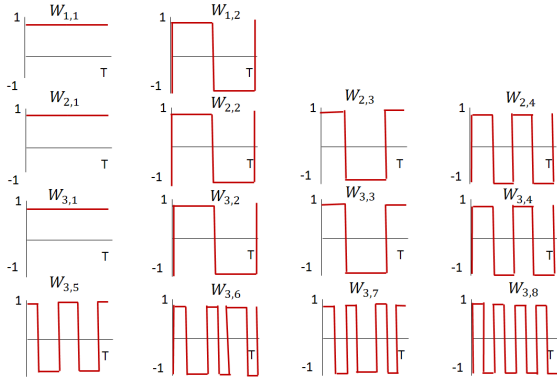


Figure 4: Walsh Hadamard functions.

Let us check this conclusion by simulation. We generate 10000 realizations of the WH-MC symbol using the Quadrature Phase-Shift Keying (QPSK) constellation diagram. We consider 64 carriers. In Fig.5, we simulate for both OFDM and WH-MC, the CCDF of the PAPR, respecting the same parameters for the two systems.

We can observe that the conventional OFDM and the WH-

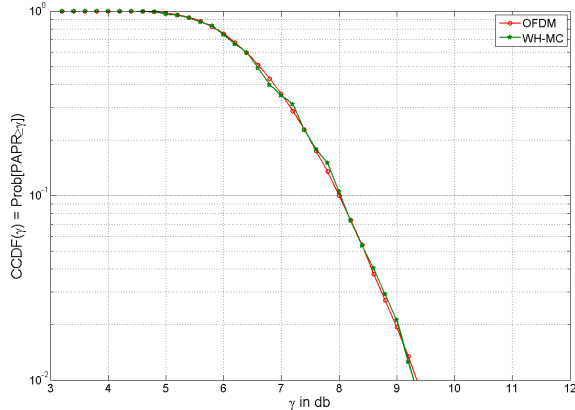


Figure 5: CCDF of the PAPR for conventional OFDM and WH-MC.

MC have the same PAPR distribution function, hence the same PAPR performance. Indeed, this observation is consistent with our theoretical predictions.

B. WCP-OFDM

Weighted Cyclic Prefix-OFDM (WCP-OFDM) is a variant of OFDM that refers to FBMC transmission system provided with short filters. WCP-OFDM can use the Out-of-Band Energy (OBE) prototype filter defined in [27] as a short filter, in this case, the family of modulation functions is expressed

as ³:

$$g_m(k) = g(k)e^{j2\pi\frac{m}{M}k} = \begin{cases} \frac{1}{\sqrt{M}}\cos(a + b\frac{2k+1}{2\Delta})e^{j2\pi\frac{m}{M}(k)} & \text{if } 0 \leq k \leq \Delta - 1, \\ \frac{1}{\sqrt{M}}e^{j2\pi\frac{m}{M}(k)} & \text{if } \Delta \leq k \leq M - 1, \\ \frac{1}{\sqrt{M}}\cos(a + b\frac{2(P-k)+1}{2\Delta})e^{j2\pi\frac{m}{M}(k)} & \text{if } M \leq k \leq P - 1, \\ 0, & \text{else.} \end{cases}$$

with $g(k)$ is the OBE short filter.

We can easily check that $g(k)$ satisfy the conditions in Eq.(2) and Eq.(3). In addition, We notice that $\forall m \in \llbracket 0, M - 1 \rrbracket$ $\forall k \in \llbracket 0, P \rrbracket$ the modulus $|g_m(k)|^2 = |g(k)e^{j2\pi\frac{m}{M}k}|^2 = |g(k)|^2$ depends on time. From Corollary.4, the PAPR performance of WCP-OFDM has to be worse than the conventional OFDM.

To approve this conclusion, we simulate the CCDF of the PAPR by considering the OBE filter.

Fig.6 represents a comparison of the CCDF of the PAPR

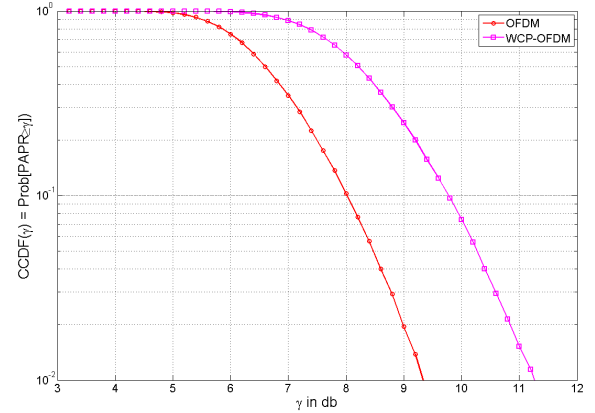


Figure 6: CCDF of the PAPR for conventional OFDM and WCP-OFDM.

between the conventional OFDM and the WCP-OFDM. We can notice that the curve of WCP-OFDM is shifted to the right, compared to OFDM. Thus, OFDM has a better PAPR performance than WCP-OFDM, which matches our theoretical result.

C. Wavelet OFDM

Wavelet OFDM, or also known as Orthogonal Wavelet Division Multiplexing (OWDM) [28], is an MCM system based on the wavelet transform. The principle of the wavelet transform is to decompose the signal in terms of small waves components called wavelets. The Wavelet OFDM transmitted signal can be defined as:

$$x(t) = \sum_{j=0}^{L-1} \sum_{k=0}^{2^J-j-1} w_{j,k}\psi_{j,k}(t) + \sum_{q=0}^{2^J-L-1} a_{L-1,q}\phi_{L-1,q}(t).$$

³ $b = \frac{1}{\alpha + \beta M_0}$, $a = \frac{\pi}{4} - \frac{1}{2}b$, $M = \Delta M_0$, $\alpha = -0.1714430594740783$, $\beta = -0.5852184808129936$, $\Delta = P - M$

- L : number of decomposition levels used,
- J : maximum number of decomposition levels,
- $W_{j,k}$: wavelet coefficients located at k -th position from scale j ,
- $a_{L-1,k}$: approximation coefficients located at k -th position from the coarsest scale $L-1$,
- $\psi_{j,k} = 2^{-j/2}\psi(2^{-j}t-k)$: the wavelet orthogonal family, ψ is the mother wavelet function,
- $\phi_{L-1,k} = 2^{-\frac{L-1}{2}}\phi(2^{-(L-1)}t-k)$: the scaling orthogonal family at the scale $L-1$, ϕ is the mother scaling function,

For more details about the wavelet theory, the reader can refer to [29].

Several wavelets can be used to modulate the input symbols, such as Daubechies, Coiflets, and Symlets. We are interested here to the Haar wavelet, which belongs to the family of Daubechies wavelets. The Haar mother wavelet function $\psi_{\text{haar}}(t)$ is expressed as:

$$\text{with } \psi_{\text{haar}}(t) = \begin{cases} 1 & \text{if } 0 \leq t \leq \frac{T}{2}, \\ -1, & \text{if } \frac{T}{2} \leq t \leq T, \\ 0, & \text{else.} \end{cases} \quad (34)$$

The scaling function $\phi_{\text{haar}}(t)$ can be described as:

$$\text{and } \phi_{\text{haar}}(t) = \begin{cases} 1 & \text{if } 0 \leq t \leq T, \\ 0, & \text{else.} \end{cases} \quad (35)$$

Fig.7 describes the first few haar wavelet functions $\psi_{j,k}^{\text{haar}}$. As

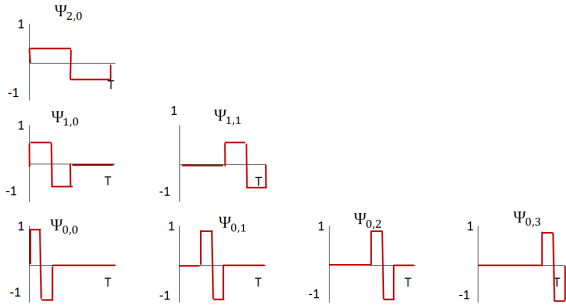


Figure 7: Haar wavelet function for different scales.

we can notice, the temporal support of some functions $\psi_{j,k}^{\text{haar}}$ is less than the symbol period T , this family of functions does not satisfy then the constraint in Eq.(2). From Property.4, we can get a better PAPR performance than using Fourier transform. Let us check it by simulation. We use Haar wavelet transform, and we extract the detail and approximation coefficients at the maximal level 6. We can observe in Fig.8 that the curve of Haar Wavelet OFDM is shifted to the left, compared to OFDM. Thus, Haar Wavelet OFDM has a better PAPR performance than the conventional OFDM.

V. CONCLUSION

In this paper, we have investigated the GWMC system based on the family of modulation functions (the modulation

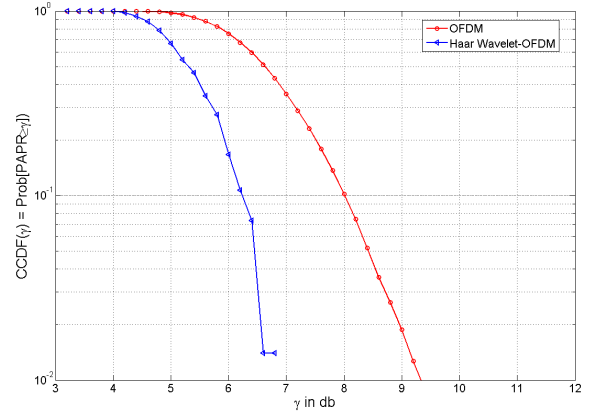


Figure 8: CCDF of the PAPR for conventional OFDM and Haar Wavelet based OFDM.

transform and the pulse shaping filter) that does not vanish in the period symbol, and we have proved analytically that the PAPR, which depends on the modulation waveform, is optimal when the sum of this waveforms over the number of carriers and the number of symbols is constant over time. We have concluded that there exists an infinite number of GWMC systems that are optimal in terms of PAPR performance, and the conventional OFDM based on the Fourier transform and the rectangular filter belongs to this family. In addition to that, we have deduced that the PAPR performance of GWMC systems cannot be better than OFDM system without reducing the temporal support of the modulation functions compared to the symbol period.

We have given some examples to illustrate our theoretical results: the WH-MC is optimal based on the characteristics of its waveform and has then the same PAPR performance as the conventional OFDM, the WCP-OFDM's waveform is not constant over time and thus it is worse than the conventional OFDM in terms of PAPR performance. We have also showed that for the Haar wavelet waveform which does not satisfy our constraints, the PAPR performance is better than the conventional OFDM with a loss in terms of frequency localization.

The future work is to construct a waveform that reduces the PAPR compared to OFDM, by acting on the number of intervals that vanish over time and taking into consideration the trade off between the PAPR and the frequency localization.

APPENDIX

We study the variations of the function $s(f) = 1 - 2f + 2fe^{-\frac{1}{f}}$, we have

$$s'(f) = -2 + 2e^{-\frac{1}{f}} + \frac{2}{f}e^{-\frac{1}{f}} \quad (36)$$

$$\begin{aligned} s''(f) &= \frac{2}{f^2}e^{-\frac{1}{f}} + 2\left(-\frac{1}{f^2}e^{-\frac{1}{f}} + \frac{1}{f} \frac{1}{f^2}e^{-\frac{1}{f}}\right) \\ &= \frac{2}{f^3}e^{-\frac{1}{f}} \geq 0 \end{aligned} \quad (37)$$

As we can see in Table IV, the function s is positive when

Table IV: Study of the positivity of the function s

f	0	f_0	$+\infty$
$s''(f)$		+	
$s'(f)$			0
$s(f)$	1	0	-1

$0 < f \leq f_0$. A numerical approximation gives $f_0 \approx 0.63$.

ACKNOWLEDGMENT

This work has received a French state support granted to the CominLabs excellence laboratory and managed by the National Research Agency in the "Investing for the Future" program under reference Nb. ANR-10-LABX-07-01. The authors would also like to thank the Region Bretagne, France, for its support of this work.

REFERENCES

- [1] R. V. Nee and R. Prasad, *OFDM for Wireless Multimedia Communications*. Inc.: Artech House, 2000.
- [2] P. Siohan, C. Siclet, and N. Lacaille, "Analysis and Design of OFDM/OQAM Systems based on Filterbank Theory," *Signal Processing, IEEE Transactions on*, vol. 50, no. 5, pp. 1170–1183, 2002.
- [3] M. Fuhrwerk, J. Peissig, and M. Schellmann, "Channel Adaptive Pulse Shaping for OQAM-OFDM Systems," *EUSIPCO*, 2014.
- [4] B. Le Floch, M. Alard, and C. Berrou, "Coded Orthogonal Frequency Division Multiplex," *Proceedings of the IEEE*, vol. 83, no. 6, pp. 24–182, 1995.
- [5] C. Siclet, P. Siohan, and D. Pinchon, "Perfect Reconstruction Conditions and Design of Oversampled DFT-modulated transmultiplexers," *EURASIP journal on applied signal processing*, vol. 2006, pp. 94–94, 2006.
- [6] W. Kozek and A. F. Molisch, "Nonorthogonal Pulses for Multicarrier Communications in Doubly Dispersive Channels," *Selected Areas in Communications, IEEE Journal on*, vol. 16, no. 8, pp. 1579–1589, 1998.
- [7] B. Farhang-Boroujeny, "Ofdm versus filter bank multicarrier," *Signal Processing Magazine, IEEE*, vol. 28, no. 3, pp. 92–112, 2011.
- [8] H. Bogucka, A. M. Wyglinski, S. Pagadarai, and A. Kliks, "Spectrally Agile Multicarrier Waveforms for Opportunistic Wireless Access," *Communications Magazine, IEEE*, vol. 49, no. 6, pp. 108–115, 2011.
- [9] A. Sahin, I. Guvenc, and H. Arslan, "A survey on Multicarrier Communications: Prototype Filters, Lattice Structures, and Implementation Aspects," 2012.
- [10] A. Aboltins, "Comparison of Orthogonal Transforms for OFDM Communication System," *Electronics and Electrical Engineering*, vol. 111, no. 5, pp. 77–80, 2011.
- [11] L. Patidar and A. Parikh, "BER Comparison of DCT-based OFDM and FFT-based OFDM using BPSK Modulation over AWGN and Multipath Rayleigh Fading Channel," *International Journal of Computer Applications*, vol. 31, no. 10, 2011.
- [12] G. D. Mandyam, "On the Discrete Cosine Transform and OFDM Systems," in *Acoustics, Speech, and Signal Processing, 2003. Proceedings.(ICASSP'03). 2003 IEEE International Conference on*, vol. 4. IEEE, 2003, pp. IV–544.
- [13] R. Kanti and M. Rai, "Comparative Analysis of Different Wavelets in OWDM with OFDM for DVB-T," *International Journal of Advancements in Research & Technology*, vol. 2, no. 3, 2013.
- [14] M. A. Gupta, M. P. Nigam, and V. Chaurasia, "A Review on Wavelet Transform as a Substitute to Cyclic Prefix Removal in FFT in OFDM," *International Journal of Engineering Sciences & Research Technology*, 2014.
- [15] A. H. Kattoush, "A Radon Slantlet Transforms based OFDM System Design and Performance Simulation under Different Channel Conditions," *ISRN Communications and Networking*, vol. 2012, p. 2, 2012.
- [16] A. Kliks, I. Stupia, V. Lottici, F. Giannetti, and F. Bader, "Generalized Multi-Carrier: An Efficient Platform for Cognitive Wireless Applications," in *Multi-Carrier Systems & Solutions (MC-SS), 2011 8th International Workshop on*. IEEE, 2011, pp. 1–5.
- [17] M. Bernhard and J. Speidel, "Multicarrier Transmission using Hadamard Transform for Optical Communications," *ITG-Fachbericht-Photonische Netze*, 2013.
- [18] A. Deshmukh and S. Bodhe, "Performance of DCT Based OFDM Communication System Working in 60 GHz Band," *International Journal of Engineering Science & Technology*, vol. 4, no. 1, 2012.
- [19] A. Skrzypczak, P. Siohan, and J.-P. Javaudin, "Peak-to-Average Power Ratio Issues for Pulse-Shaped Multicarrier Modulations," in *Advances on processing for multiple carrier schemes: OFDM & OFDMA*, F. Bader and N. Zorba, Eds. Nova Science Publishers, Inc., 2011, pp. 43–90.
- [20] A. Kliks, "New Transmission and Reception Techniques of the Generalized Multicarrier Signals," Ph.D. dissertation, Poznan University of Technology, 2011.
- [21] M. Chafii, J. Palicot, and R. Gribonval, "Closed-form Approximations of the PAPR distribution for Multi-Carrier Modulation Systems," *Eusipco, Lisbon, Portugal*, 2014.
- [22] —, "Closed-form Approximations of the Peak-to-Average Power Ratio Distribution for Multi-Carrier Modulation and their Applications," *EURASIP Journal on Advances in Signal Processing*, vol. 2014, no. 1, pp. 1–13, 2014.
- [23] S. Boyd and L. Vandenberghe, *Convex optimization*. Cambridge university press, 2004.
- [24] N. De Bruijn, "Uncertainty Principles in Fourier Analysis," *Inequalities*, vol. 2, pp. 57–71, 1967.
- [25] M. Chafii, J. Palicot, and R. Gribonval, "A PAPR Upper Bound of Generalized Waveforms for Multi-Carrier Modulation Systems," *ISCCSP, 6th International Symposium on Communications, Control and Signal Processing, Athens, Greece*, 2014.
- [26] B. Evans *et al.*, "Hardware Structure for Walsh-Hadamard Transforms," *Electronics Letters*, vol. 34, no. 21, pp. 2005–2006, 1998.
- [27] D. Roque, "Modulations Multiporteuses WCP-OFDM: évaluation des performances en environnement radiomobile," Ph.D. dissertation, Université de Grenoble, 2012.
- [28] S. L. Linfoot, M. K. Ibrahim, and M. M. Al-Akaidi, "Orthogonal Wavelet Division Multiplex: An Alternative to OFDM," *Consumer Electronics, IEEE Transactions on*, vol. 53, no. 2, pp. 278–284, 2007.
- [29] S. Mallat, *A Wavelet Tour of Signal Processing*. Academic press, 1999.